ADVANCES IN ATMOSPHERIC SCIENCES, VOL. 29, NO. 2, 2012, 307–319

Using Synoptic Classification and Trajectory Analysis to Assess Air Quality during the Winter Heating Period in Ürümqi, China

WANG Lili[1] (王莉莉), WANG Yuesi*[1] (王跃思), SUN Yang[1] (孙 扬), and LI Yuanyuan[2] (李圆圆)

[1]*State Key Laboratory of Atmospheric Boundary Layer Physics and Atmospheric Chemistry, Institute of Atmospheric Physics, Chinese Academy of Sciences, Beijing* 100029

[2]*Xinjiang Weather Office, Ürümqi* 830002

(Received 12 January 2011; revised 27 May 2011)

ABSTRACT

Synoptic patterns identified by an automated procedure employing principal- component analysis and a two-stage cluster analysis, and backward trajectory analysis clustered by the HYSPLIT4.9 model were used to examine air quality patterns over Ürümqi, China, one of the most heavily polluted cities in the world. Six synoptic patterns representing different atmospheric circulation patterns and air-mass characteristics were classified during the winter heating periods from 2001 to 2008, and seven trajectory clusters representing different paths of air masses arriving at Ürümqi were calculated during the winter heating periods from 2005 to 2008. Then air quality was evaluated using these two approaches, and significant variations were found across both synoptic patterns and trajectory clusters. The heaviest air-pollution episodes occurred when Ürümqi was either in an extremely cold, strong anticyclone or at the front of a migrating cyclone. Both conditions were characterized by with light winds, cold, wet surface air, and relatively dry upper air. Ürümqi was predominately influenced by air masses from the southwest and from local areas. Air pollution index (API) levels were highest for air masses originating from the southwest with a longer path or for the local area, because of transport from semi-desert/desert regions by strong winds and because of local heavy pollution emissions, respectively. The interactions between these two analytical approaches showed that poor diffusion conditions, together with local circulation, enhanced air pollution, besides, regional air-mass transport caused by strong winds contributed to serious air quality under relatively good diffusion conditions.

Key words: synoptic climatology, backward trajectory, automated meteorological classification, air pollution index (API), Ürümqi

Citation: Wang, L. L., Y. S. Wang, Y. Sun, and Y. Y. Li, 2012: Using synoptic classification and trajectory analysis to assess air quality during the winter heating period in Ürümqi, China. *Adv. Atmos. Sci.*, **29**(2), 307–319, doi: 10.1007/s00376-011-9234-4.

1. Introduction

Ürümqi, the city farthest from sea in the world, is located in northwestern China in the hinterland of the Eurasian continent. It is the capital of the Xinjiang Uygur Autonomous Region, which is situated in the northern foothills of the Tianshan Mountains at an altitude of ∼680–920 meters above sea level. To the north is the Junggar Basin, and in the other three directions it is surrounded by mountains. Ürümqi has an arid climate and is located in a semi-desert/desert region (Fig. 1). In recent years, with industrialization and rapid urban growth, the urban air quality has gradually deteriorated, and Ürümqi has become the most polluted city in the world (Mamtimin and Meixner, 2007; Li et al., 2008). The level of air pollution has seriously affected sustainable socioeconomic development and human health (Mao, 1997; Wang and Wang, 2007). Situated upstream of the Asian dust passage, the pollutants from Ürümqi are transported to other places such as central and eastern China (Kaiser and Qian, 2002; Yuan et al., 2006; Xin

*Corresponding author: WANG Yuesi, wys@mail.iap.ac.cn

© China National Committee for International Association of Meteorology and Atmospheric Sciences (IAMAS), Institute of Atmospheric Physics (IAP) and Science Press and Springer-Verlag Berlin Heidelberg 2012

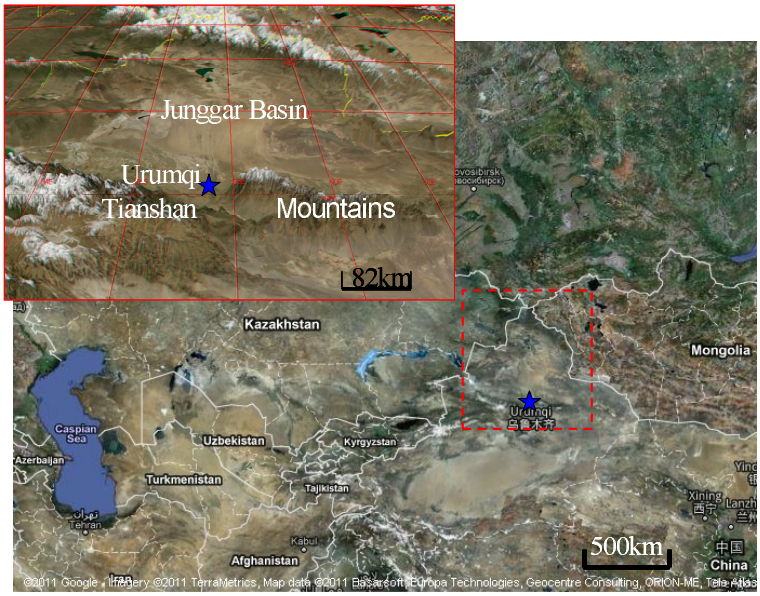

Fig. 1. Topography and location map of Ürümqi.

et al., 2010). Compared to other seasons, the heaviest urban-pollution episodes occur during the winter heating period, due to the combustion of coal used for heating homes and buildings during the winter, and the unfavorable dispersion due to geographical and meteorological conditions (Huang, 2005; Guo et al., 2006; Wang et al., 2008).

Emission sources and weather situations contribute to different types of air quality in general, but in an urban environment, serious pollution episodes mainly result from unfavorable air dispersion due to weather conditions (Ziomas et al., 1995). Meteorological conditions affect air pollution in numerous ways, such as air-mass transport, chemical transformation, and removal of pollutants via wet and dry processes (Comrie, 1996; Sun et al., 2010). Backward trajectory analysis is commonly used to examine the relationship between air-mass transport and air quality (Cape et al., 2000; Eneroth et al., 2003). However, trajectories are primarily calculated from the observed wind and/or air pressure fields, and air quality is influenced by the whole air mass, which represents the sum of all meteorological variables (Lam and Cheng, 1998; Cheng et al., 2007). Synoptic classification that includes wind and thermal and moisture meteorological variables is an effective method that has been commonly used to analyze and predict impacts of weather and climate on air pollution (Davis and Kalkstein, 1990; Cheng et al., 2007).

Synoptic weather classification procedures can be divided into two distinct approaches: subjective and objective (Yarnal, 1993). The former is a qualitative and semi-quantitative approach that uses manual classification based on general circulation patterns (Kim Oanh et al., 2005), which may be biased, and focuses on hydrodynamic criteria. The latter approach is quantitative and automated and uses both thermodynamic and hydrodynamic variables (Davis and Kalkstein, 1990). In this study, we developed an objective scheme to classify the synoptic situations representing the primary and recurring states of air pollution over Ürümqi.

The objective of this study was to examine, both separately and in combination, the relationship between synoptic patterns or backward trajectories and air quality during the winter heating periods (from 15 October to 15 April the following year) from 2001 to 2008 over Ürümqi. This procedure has the potential to enable the forecast of air-pollution concentrations and the issuance of public warnings for serious weather and air-pollution situations.

2. Data and methods

2.1 *Meteorological data and selection*

Surface and upper-air meteorological data and all synoptic maps during the winter heating months from 2001 to 2008 were obtained from the Meteorological Bureau of Xinjiang Uygur Autonomous Region. For classifying synoptic patterns capable of representing synoptic-scale situations at certain moments in time, the selection of suitable weather elements is very important. In previous studies, surface and upper-air meteorological variables such as temperature, dew point or relative humidity, sea-level pressure, total cloud cover or solar total radiation, wind speed, and wind

direction have been commonly used to analyze the impact of synoptic climatology on air pollution (Davis et al., 1998; Cheng et al., 2007). In addition, visibility and total solar radiation or insolation are sometimes included (McGregor and Bamzelis, 1995).

The primary pollutants during the winter heating period are sulfur dioxide (SO_2) and particulate matter $\leqslant$10 μm (PM_{10}). To consider the impacts of Ürümqi's specific topography and meteorological variables on these pollutants in the development of the synoptic index, we used the surface values of air temperature (°C), dew point (°C), sea-level air pressure (hPa), west–east wind component (u; m s^{-1}), south–north wind component (v; m s^{-1}), total cloud cover (tenths), visibility (km) at 0200, 0800, 1400 and 2000 LST, daily total solar radiation (J m^{-2}), sunshine duration (h), and rainfall (mm) at the ground surface as well as temperature, dew point, u and v at 0800 and 2000 LST at 850 hPa. Surface meteorological variables were complete, while 8.1% of the 850-hPa data was missing. Because a complete data matrix is needed for the principal-component analysis (PCA) procedures, all missing values were estimated using one of two methods used by Bower et al. (2007): (1) for less than three consecutive days of missing data, a linear fill based on the two observations flanking the data gap, or (2) for other missing data, the long-term average value for that day. The final dataset contained 57 174 observations, or 39 variables per day over 1466 days.

2.2 *Backward trajectory calculation*

The individual backward trajectories were calculated using the HYSLPIT4.9 model from NOAA Air Resources Laboratory (http://ready.arl.noaa.gov/HYSPLIT.php) and the meteorological data from the NCEP Global Data Assimilation System (GDAS; 1°×1°). The trajectory endpoint was located at 43.44°N, 87.79°E, with a height of 100 m above the ground level [i.e., within the mixed layer (Yang et al., 2010)]. Because data from GDAS are available from December 2004 onward and because the comparison of the trajectories calculated using data from GDAS and NCEP/NCAR Global Reanalysis Data Archive (2.5°×2.5°) during an overlapping period (1 January 2006–31 April 2006) shows a statistically significant difference, we calculated the 3-day backward trajectories at 1400 LST during the winter heating periods from 2005 to 2008 using the spatially finer data from GDAS. The ideal cluster numbers were determined by the total spatial variance (TSV). The ensembles of trajectories are more representative of the path of an air parcel, and backward trajectories have been commonly used in air-quality research (Cape et al., 2000; Eneroth et al., 2003).

2.3 *Air-pollution index (API) data and analysis*

The air-pollution index (API) is a quantitative measure describing air-pollution levels in China based on the conversion of air-pollution data, mainly PM_{10}, SO_2, and nitrogen dioxide (NO_2) concentrations, into a single value ranging from 0 to 500 (Yu, 2000). The API is divided into five ranks representing different air-quality levels with respect to their impacts on human health. The first and second air-quality levels, (I: API = 0–50 and II: API = 51–100), represent good air quality and no human-health risk. The third level (III: API = 101–200) indicates light pollution affecting human health to some degree. The fourth and fifth levels (IV: API = 201–300) and (V: API > 300) denote heavy pollution and serious effects on human health. Table 1 lists breakpoint air-pollutant concentrations corresponding to the API index (SEPA, 1996). The sub-index of all kinds of pollutants (I_i) can be calculated in accordance with the sublinear Eq. (1), and the maximum sub-index among all the pollutants is then selected as the API of the city as described by Eq. (2):

$$I_i = [(C_i - C_{i,j})/(C_{i,j+1} - C_{i,,j})]\times (I_{i,j+1} - I_{i,j}) + I_{i,j} (C_{i,j} \leqslant C_i \leqslant I_{i,j+1}) , \quad (1)$$

$$\mathrm{API} = \max(I_l, I_2, \ldots, I_n) , \quad (2)$$

where C_i is the concentration of pollutant i, $I_{i,j}$ is the sub-index at the breakpoint j of pollutant i, $I_{i,j+1}$ is the sub-index at the j+1 breakpoint of pollutant i, $C_{i,j}$ is the corresponding concentration at the breakpoint j of pollutant i, $C_{i,j+l}$ is the corresponding concentration at the breakpoint j+1 of pollutant I, where the sub-index ($I_{i,j}$) and the corresponding concentration($C_{i,j}$) at the breakpoint j of pollutant i are determined using Table 1.

The API data of the study region were downloaded-

Table 1. Breakpoint air-pollutant concentrations corresponding to API data.

	Pollutant concentrations (daily average) (μg m^{-3})		
API	SO_2	NO_2	PM_{10}
50	50	80	50
100	150	120	150
200	800	280	350
300	1600	565	420
400	2100	750	500
500	2620	940	600

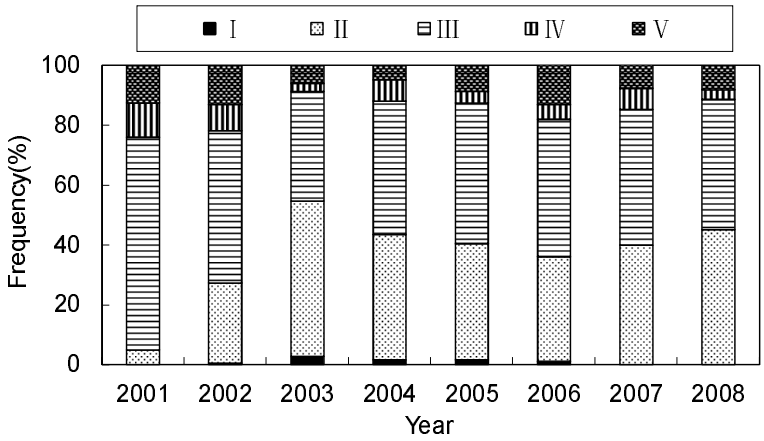

Fig. 2. Frequency for different air quality levels during the winter heating period (15 October–15 April 15) from 2001 to 2008 at Ürümqi.

from the website of the Ministry of Environmental Protection of China. Figure 2 shows frequencies for different air-quality levels during the winter heating periods from 2001 to 2008, which indicate that Ürümqi is suffering from serious air pollution. Frequencies of air quality at levels I and II were 27%–55% each year, except for 2001 (5%). The overall frequency of air quality at levels III, IV, and V was 64%, and the frequency of levels IV and V was 15% during winter heating periods from 2001 to 2008. Notably, there were 35 days with an API of 500. The major pollutants during the winter heating period are SO_2 and PM_{10}. PM_{10} is the more concentrated pollutant during heavy pollution episodes, mainly because of the large emissions from coal heating and unfavorable dispersion due to geographical and meteorological conditions (Huang, 2005; Guo et al., 2006; Wu et al., 2008).

2.4 *Methods*

A synoptic classification was established to analyze the relationships between air pollution and climatological conditions during winter heating periods in Ürümqi. PCA and a two-stage cluster analysis were used to classify days into meteorological homogenous synoptic categories (Davis and Walker, 1992; Bower et al., 2007). PCA is a commonly used multivariate statistical technique that reduces a large set of intercorrelated variables into a smaller set of linearly independent principal components (Jolliffe, 2002). The first component explains the highest proportion of the total variance in the dataset, and the last explains the lowest. Considering the units of meteorological variables, a correlation matrix was used as the input into the PCA procedure. Then, the scree test was used to select the number of components explaining the highest amount of variance (Cattell, 1966). Finally, component scores were calculated for each day. Next, a two-stage clustering technique was used to cluster the resulting component scores to produce the classification. First, Ward's clustering method, a hierarchical agglomerative method, was used to determine the number of clusters through examination of the pseudo-F and pseudo-t^2 statistics (Eder et al., 1994), which showed superiority over the average-linkage and centroid methods for this dataset. The mean conditions within each cluster were calculated and then used as inputs into k-means clustering, a nonhierarchical iterative method, to classify the final synoptic patterns.

To compare backward trajectories and synoptic patterns with respect to air quality, each trajectory cluster was linked to the synoptic pattern observed on the day the trajectory terminated, as suggested by Davis et al. (2010).

3. Results and discussion

3.1 *Synoptic climatology results using PCA and cluster analysis*

For the selected subset of 39 meteorological variables over 1466 days during the winter heating period, the PCA produced the first eight components, which explained 69% of the total variance in the raw dataset (Table 2). The variables with high loading (>0.4) for

Table 2. Statistics for the first eight principal components.

	PC1	PC2	PC3	PC4	PC5	PC6	PC7	PC8
Eigenvalue	10.88	4.73	3.03	2.08	1.86	1.59	1.41	1.34
Explained variance (%)	27.91	12.12	7.78	5.34	4.78	4.08	3.62	3.45
Cumulative variance (%)	27.91	40.03	47.81	53.14	57.92	62	65.62	69.07

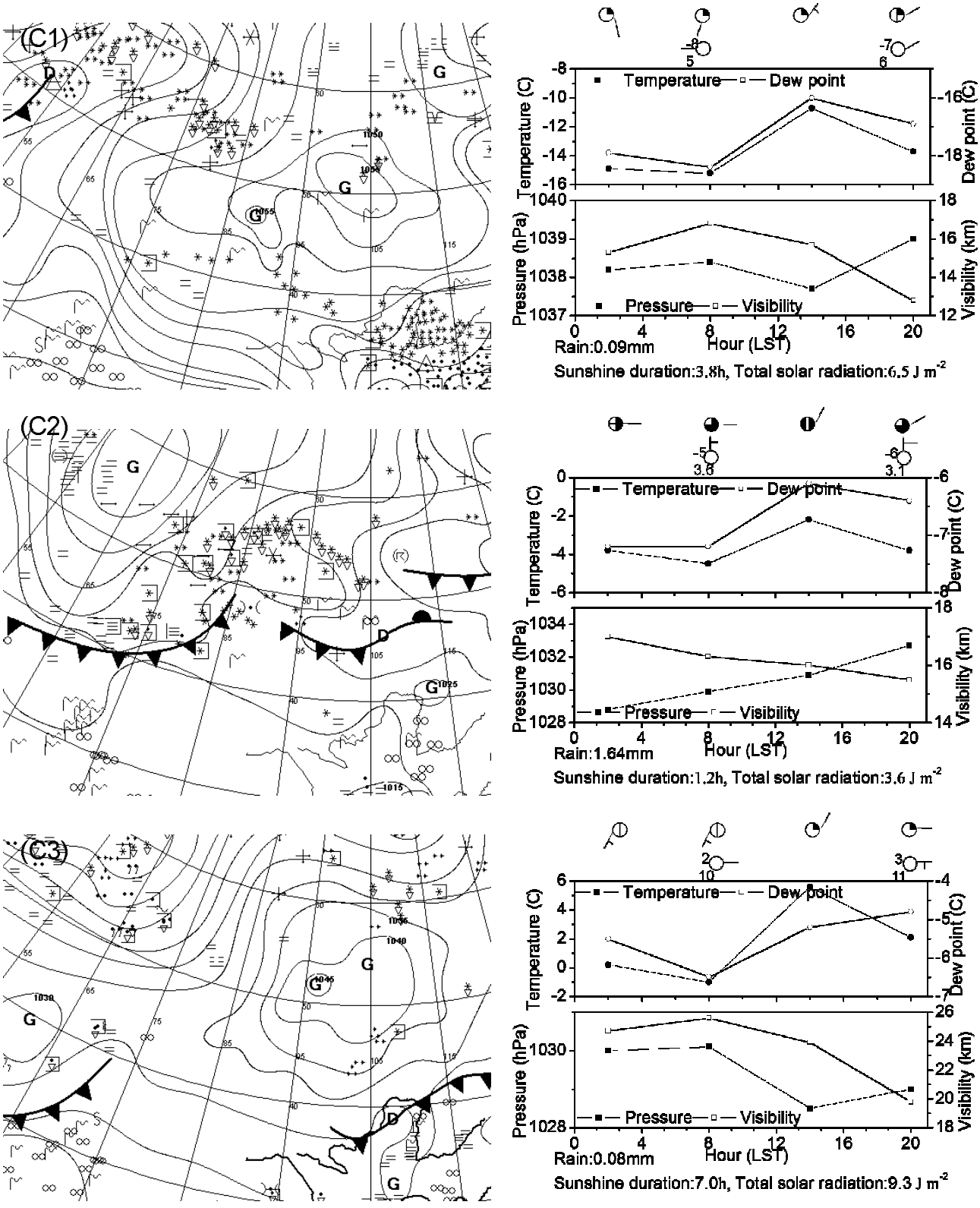

Fig. 3. Surface synoptic maps for the day closet to each of the cluster centroids (left), and average meteorological variables for the six-synoptic clusters from 2001 to 2008 (right). Total cloud cover, wind speed and direction (surface and 850 hPa), 850-hPa temperature and dew-point depression were represented by standard station symbols.

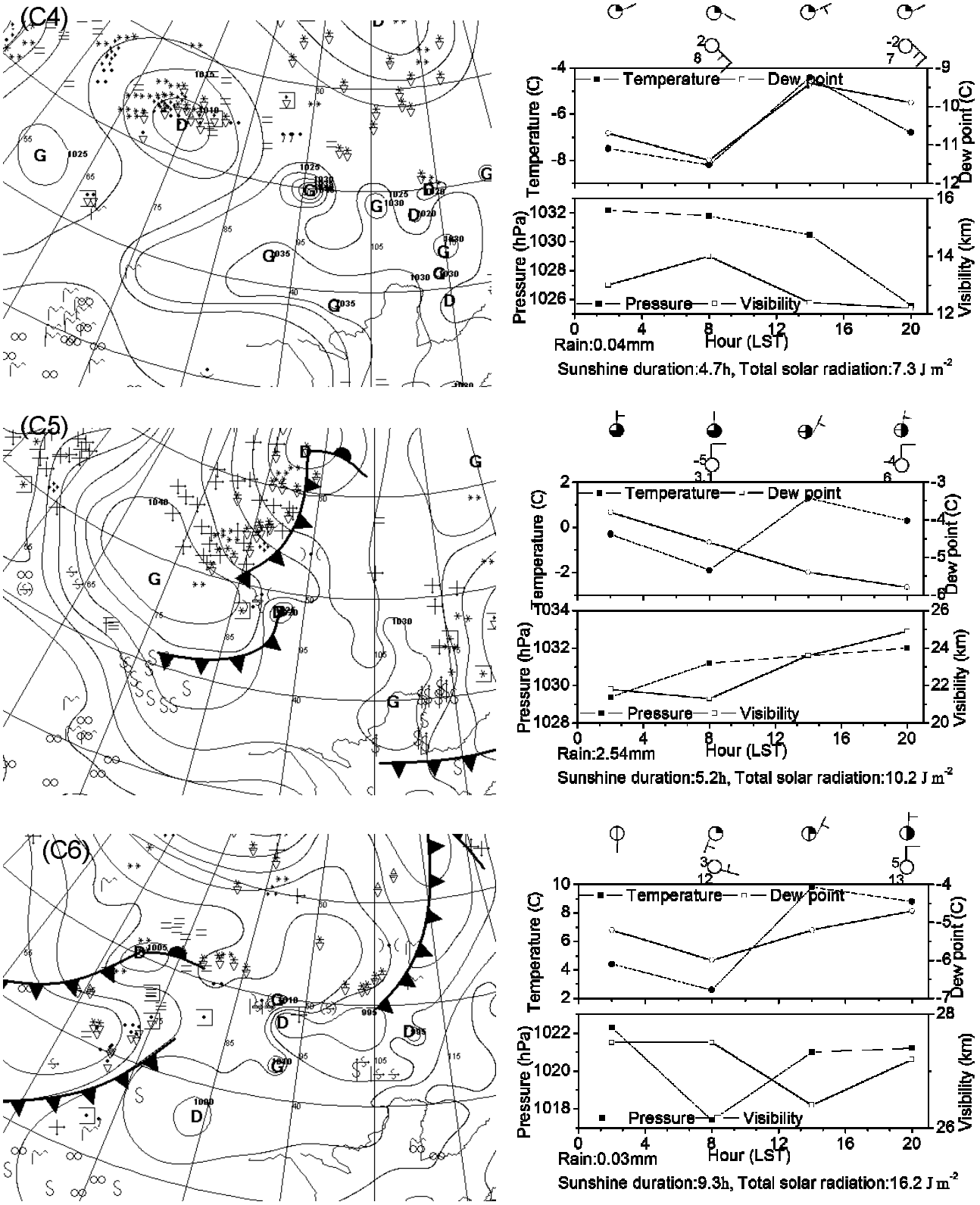

Fig. 3. (Continued).

Table 3. Monthly and annual cluster frequencies (number of days) over the 8-year study period (2001–2008).

	Synoptic types					
Month	C1	C2	C3	C4	C5	C6
Jan	130	50	21	44	3	0
Feb	82	47	24	45	18	10
Mar	15	33	29	25	46	100
Apr	0	11	6	0	29	74
Oct	0	16	77	5	19	19
Nov	6	62	100	44	18	10
Dec	101	65	34	41	7	0
Year	C1	C2	C3	C4	C5	C6
2001	49	32	26	20	25	31
2002	38	33	33	23	28	28
2003	52	29	26	26	28	22
2004	32	47	34	33	19	19
2005	54	41	32	27	11	18
2006	31	45	44	26	7	30
2007	26	31	51	29	14	32
2008	52	26	45	20	8	33

PC1 were sea-level pressure, surface temperature and dew point, visibility, sunshine duration, and solar total radiation, which represent the dynamic, thermal, moisture, and radiation characteristics of the air mass over Ürümqi on these days. PC2 included high-loading variables for total cloud cover, surface northerly wind in the morning, rainfall, solar total radiation, sunshine duration, and 850-hPa u and v components at night, which represent the moisture and radiation characteristics. PC3 and PC4 included 850-hPa thermal, moisture, and wind variables in the morning and 850-hPa thermal and moisture variables at night, respectively. PC5 included surface westerly wind in the morning and 850-hPa thermal and moisture variables at night. PC6 and PC8 included surface easterly winds in the morning and surface southerly winds in the afternoon, respectively. PC7 included surface northerly winds in the morning and 850-hPa winds at night.

Component scores for each day were calculated, and then a 1466×8-component score matrix was produced and was grouped using a two-stage clustering technique. Finally, six clusters representing six meteorologically homogeneous patterns were classified. To determine the identity of each synoptic class, means for each of the 39 meteorological variables were calculated for each cluster. Synoptic charts for the day closest to each of the cluster centroids and average meteorological variables for the six-synoptic clusters are presented in Fig. 3; monthly and annual frequencies for the six clusters are also provided in Table 3.

Cluster 1 (C1; number of days = 334, 22.8% of study period), the most prevalent synoptic cluster, captured the center of a stationary high-pressure system that extended from a Western Siberian or Mongolian high-pressure zone (Fig. 3: C1). C1 was the most prevalent synoptic pattern in winter, which is consistent with the findings by Wu et al. (2007). C1 was characterized by the coldest surface and upper air, highest pressure, relatively high moisture at the surface (i.e., the dew-point depression was small), light wind, and lower visibility and solar radiation. In addition, surface wind as rather weak (except 1400 LST wind, which was somewhat strong from the northeast), and the upper westerly or northeasterly wind was also weak. This synoptic pattern occurred most often in December, January and February, and the annual frequency of this cluster was highly variable over the 8-year period, ranging from only 25 days to 54 days (Table 3).

Cluster 2 (C2; 284 days, 19.4%) captured pre-cold-front and cold-front passages and was sometimes followed by C3 and C5 (Fig. 3: C2, and Table 4), with increasing pressure and cloud cover. C2 was characterized by the third-lowest temperatures and highest humidity at the surface and in the upper air, a small amount of precipitation, and the lowest solar radiation. Remarkably, the wind was rather low from the eastern or northeastern flow at the surface and from the north in the upper layer. C2 occurred most often in November, December, January, and February, and the annual frequency of C2 conditions ranged from 26 to 47 days (Table 3).

Cluster 3 (C3; 291 days, 19.8%) characterized the center of a moderate anticyclone or the backside of a Mongolian high-pressure zone (Fig. 3: C3). C3 was characterized by second-highest surface and upper-air temperatures, moderate pressure, the second-lowest moisture at the surface and in the upper air, the second-greatest visibility and solar radiation, and the lowest amount of cloud cover. The dry air and low cloud cover, which allow maximum nocturnal radiation cooling, resulted in a large diurnal temperature variation and well-developed air mixing by day. The

Table 4. Development of synoptic patterns with time, 8 years of winter heating periods (2001–2008).

	Synoptic types					
Following types	C1	C2	C3	C4	C5	C6
C1	217	34	18	43	19	3
C2	43	108	44	47	16	5
C3	21	49	130	26	39	26
C4	41	30	56	68	4	5
C5	8	51	13	4	28	36
C6	4	12	29	16	34	118

relatively stronger surface wind was from the southwest to the northeast, and the weak upper wind was from the east. C3 occurred most often in October and November, and the annual frequency ranged from 26 to 51 days (Table 3).

Cluster 4 (C4; 204 days, 13.9%) occurred when Ürümqi was at the front of a migrating cyclone (Fig. 3: C4). The surface-pressure decreases; surface temperature and dew point were the second lowest. C4 was also characterized by wet surface air, dry upper air, weak surface winds mainly from the east or northeast, and strongest upper winds mainly from the southeast, the third-least solar radiation, and the lowest visibility. C4 conditions occurred most often in November, October, January, and February, and the annual frequency ranged from 20 to 33 days (Table 3).

Cluster 5 (C5; 140 days, 9.6%) the lowest-occurring synoptic cluster, captured cold-front and post-cold-front passages (Fig. 3: C5). The front either quickly passed Ürümqi and was replaced by other clusters (Table 4: C3 and C6) or was blocked off by the Tianshan Mountains and remained stable for some period. C5 was characterized by the most precipitation, the strongest winds from the north, relatively warm and wet surface air, cold and wet upper air, the second-greatest cloud cover, and the second-highest visibility and solar radiation. C5 occurred most often in March and April, and the annual frequency ranged from 7 to 28 days (Table 3).

Cluster 6 conditions (C6; 213 days, 14.5%) occurred when Ürümqi was in the center of a weak anticyclone or at the front of a migrating anticyclone (Fig. 3: C6). This cluster was steady or was followed by C5 (Table 4). C6 was characterized by the warmest and driest surface and upper air, the greatest visibility and solar radiation, high surface winds from south to north, and high upper winds from east to north. Due to the clear sky conditions and high temperatures, mixing was well developed in the daytime, and a large diurnal temperature variation occurred. C6 conditions occurred most often in March and April, and the annual frequency ranged from 18 to 33 days (Table 3).

To analyze the development of the clusters with time, the sequence of day-by-day occurrence for the six clusters was examined (Table 4). Except for C4 and C5, each cluster had a high frequency of repetition, which indicated the persistence of the synoptic situations. However, synoptic systems characterized as C4 and C5 moved fast and were quickly replaced by other clusters.

3.2 *Application of synoptic climatology results to air-quality evaluation*

The API statistics for Ürümqi during the winter heating period for each of the six identified synoptic patterns were calculated (Fig. 4 and Table 5) to examine the critical impact of meteorological conditions on accumulation and deposition of air quality. Because the result of the test of homogeneity of variance showed that the variance within each of the clusters was unequal, a nonparametric, two-sided Kolmogorov-Smirnov test was utilized to test the differences between the cumulative distribution functions of the mean API associated with each cluster. Results indicated that 14 of 15 possible cluster combinations exhibited statistically different API distributions at a 5% significance level, except the C1/C4 combination.

Remarkably, C4 and C1 conditions were associated with the highest mean API values of 206 and 197; C2 and C3 conditions were associated with the moderate means of 135 and 121; and C6 and C5 conditions were associated with the lowest means of 100 and 96. Considering the overall contribution (defined as the normalized product of the cluster frequency and the mean API; Table 5), C1 and C4 had the largest API contributions at 31.6% and 20.1%, respectively. Although

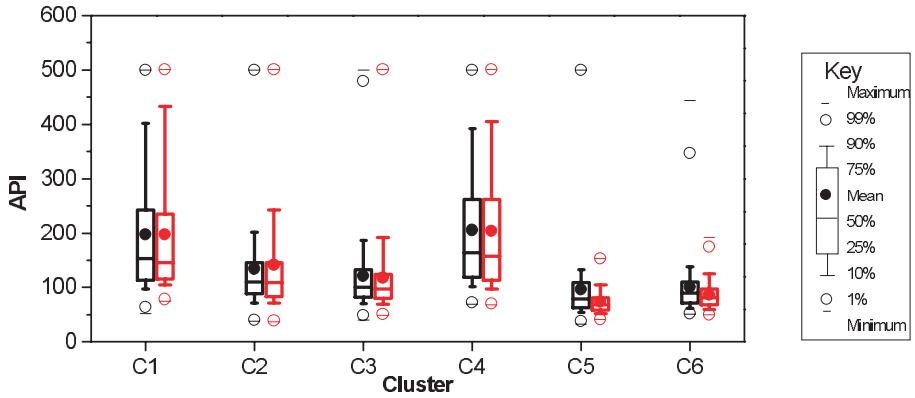

Fig. 4. Box plots of API associated with the six synoptic patterns. The black plots represented the results from 2001 to 2008, and the gray ones from 2005 to 2008.

Table 5. Summary statistics of API data in Ürümqi associated with different synoptic patterns for 8 years of winter heating periods (2001–2008).

Synoptic Patterns and frequency (%)	Mean and standard deviation of API	Percentage (%) of API > 100	Percentage (%) of API > 200	Normalized contribution*
C1 (22.8%)	197±118	87.7	29.0	31.6
C2 (19.4%)	135±85	64.8	10.2	18.3
C3 (19.8%)	121±70	50.2	7.6	16.8
C4 (13.9%)	206±116	90.7	33.3	20.1
C5 (9.6%)	96±67	33.6	3.6	6.4
C6 (14.5%)	100±49	35.2	2.3	10.2

Note: *Normalized contribution of the six clusters to the API values.

C4 had a lower frequency (13.9%), the highest average API value led to a higher contribution. Moderate contributions from C2 and C3 were associated with moderate average API values. The lowest contributions were from C5 and C6, which were limited with respect to both their frequencies and average API values. The percentages of days with API > 100 were the highest for C4 and C1 (90.7% and 87.7%, respectively) and the lowest for C6 and C5 (35.2% and 33.6%, respectively). However, the days with API >200 occurred mainly with C4 and C1 conditions (33.3% and 29.0%, respectively); other clusters had fewer of these heavily polluted days. The mean API values for these six clusters in different seasons showed similar trends (Fig. 5), but there was a seasonal change, with higher API values in December, January and February, and lower API values in March, April, and October. This change occurred because of relatively good diffusion conditions and less pollution emissions (Wu et al., 2007).

Cluster 4, the synoptic pattern associated with the most pollution, was associated with the extreme pollution episodes attributable to difficult conditions for pollutant dispersion. The preceding part of a low-pressure cyclone usually resulted in high pollution (Chen et al., 2008). Lower air temperature and dew point (the second lowest among the six clusters), as well as wet surface air, dry upper air, weak wind and less precipitation, caused the pollution generated by local sources to accumulate and made dispersion difficult. In addition, in this synoptic situation, a dense inversion layer was created, which led to further difficulty in dispersing pollutants. A weak surface wind from the northeast and a high upper wind from the southeast were both associated with heavy pollution, which supports the earlier finding by Wu et al. (2007, 2008) that heavy pollution emissions occur to the southwest, south, and southeast of Ürümqi.

Cluster 1, the second-most polluted and the most prevalent synoptic pattern, describes the highest-pressure and stationary anticyclone over Ürümqi, which supports earlier findings by Huang (2005). The subsidence flow caused by a high-pressure system was unfavorable for the dispersion of pollutants (Chen et al., 2008). Simultaneously, the lowest air temperature and dew point, higher surface humidity, lower upper-air humidity, and weak wind led to a dense inversion layer, which was crucial to the formation of severe pollution conditions. This synoptic pattern, which had

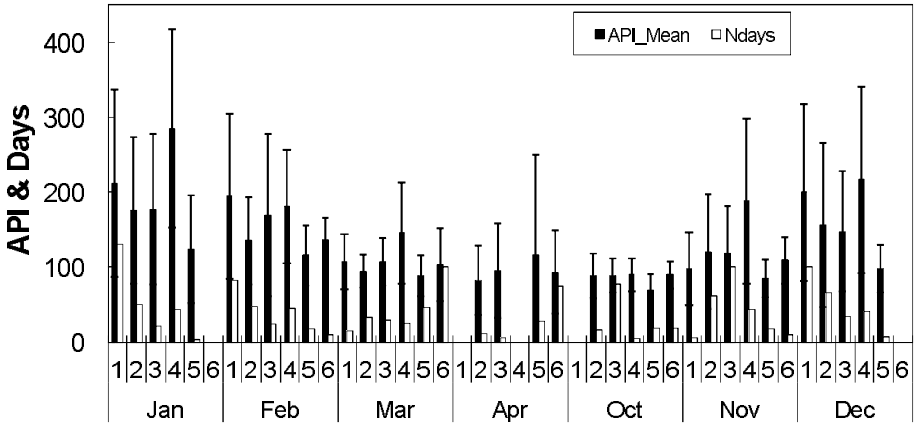

Fig. 5. Mean API values and number of days for different synoptic clusters in different months (2001–2008). Bars represent the standard deviations of API values.

both the highest frequency (22.8%) and highest contribution to the API (31.6%), was the main synoptic weather pattern contributing to severe pollution in Ürümqi.

Cluster 2 ranked third in pollution levels, with a weak wind, lower temperature and the lowest solar radiation and highest cloud cover. As pre-cold front and cold-front passages move through Ürümqi, the unstable weather conditions generate moderate precipitation, which helps to deposit pollutants. However, a small amount of rain or snow is not enough to clean the air (Li and Wang, 2007); furthermore, weak wind, especially from the east or northeast, is unfavorable for dispersion (Wu et al., 2008).

The surface synoptic conditions of Cluster 3 were associated with a moderate high-pressure system over Ürümqi. Though the subsidence flow caused by the high-pressure system was unfavorable for dispersion, vertical atmospheric movement and increased surface radiative inversion were associated with relatively warmer and drier air, the least cloud cover, and stronger winds, which were favorable for some degree of dispersion.

Synoptic Clusters 6 and 5 were associated with to the lowest API. A better dispersion situation was associated with C6, which depicted weak anticyclone or the preceding part of an anticyclone with the warmest and driest air both at the surface and in the upper layer, as well as lower cloud cover and a moderate wind, which is consistent with the findings by Huang (2005). C5, which captured cold-front and post-cold-front passages, was associated with strong wind and greater precipitation, which helped to disperse pollutants. However, due to the strong winds from the north, dust was brought into Ürümqi, leading to heavy dust pollution in the spring (Wang et al., 2002; Huang, 2005; Wu et al., 2007). Thus, 3.6% of the days in C5 had air quality with API > 200 (Table 5), with a larger standard deviation for C5 in April (Fig. 5).

3.3 *Synoptic pattern/trajectory and air-quality interactions*

First, to examine the transport of air pollution over a longer range, a total of 733 3-day backward trajectories were calculated and clustered, and API values were grouped according to the trajectory clusters (Fig. 6). The results showed that Ürümqi was predominately influenced by air masses from the southwest. Nearly 69% of air masses were from the southwest, ~22% were from the local area, and 9% were from

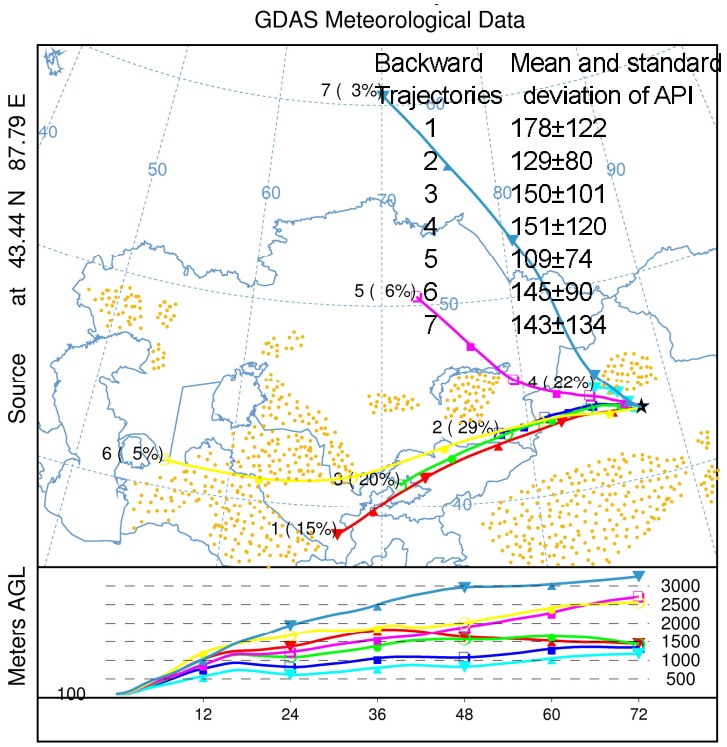

Fig. 6. Mean backward trajectory clusters during the heating period from 2005 to 2008 at Ürümqi, and mean and standard deviation of API according to the trajectory clusters. The dots represents deserts.

the northwest. For southwesterly flows, API levels were much higher for clusters with longer trajectories, because of transport from semi-desert/desert regions with strong winds. Trajectory cluster 4 was associated with local flow and circulation and a relatively high API level (151), which showed local heavy pollution sources. Trajectory clusters 6 and 7, making a contribution of only ∼8%, were the longest trajectories from the southwest and northwest, respectively, with moderate API levels. Air masses of these clusters moved fast and carried some dust into Ürümqi, sometimes contributing to heavy pollution. Trajectory cluster 2 and 5 were the shortest trajectories from southwest and northwest, respectively, with relatively good air quality, attributable to less transport and good dispersion conditions associated with moderate winds.

To compare them with the results of backward trajectory analysis, API distributions associated with the six synoptic patterns during the overlap period from 2005 to 2008 are shown in Fig. 4. This comparison shows similar trend to the results from 2001–2008.

The results for interactions between synoptic patterns and trajectory clusters are shown in Fig. 7. Overall, mean API values were highest for C1 and C4, moderate for C2 and C3, and lowest for C5 and C6 regardless of the trajectories, which demonstrates that the API levels were mainly decided by synoptic patterns. However, the API levels were somewhat different according to different trajectories for different synoptic patterns. Backward trajectory clusters 5, 6, and 7 only made a contribution of ∼14%, and less sample days might have caused some errors; thus, the analysis was focused on the interaction between synoptic patterns and trajectory clusters 1–4. Generally, trajectory cluster 1 was associated with the highest API levels for different synoptic patterns due to transport from semi-desert/desert regions (except C1 with the highest API value for trajectory cluster 4). Mean API values for C1 varied from 189 to 227. Because C1 was associated with a synoptic situation commonly linked to a cold, strong, and stationary anticyclone, and trajectory cluster 4 represents air mass from the local area, these results demonstrate that air pollution is enhanced via local accumulation and recirculation. The API value was second highest for trajectory cluster 4 for C4, because C4 was associated with poor diffusion conditions, and air pollution is heavy when air masses are from the local area. The diffusion conditions for C2, C3, C5, and C6 were much better than those of C1 and C4, thus, air pollution caused by local circulation was not so heavy compared with regional transportation associated with strong winds. For C6, there was no significant difference among different trajectory clusters, due to good diffusion conditions.

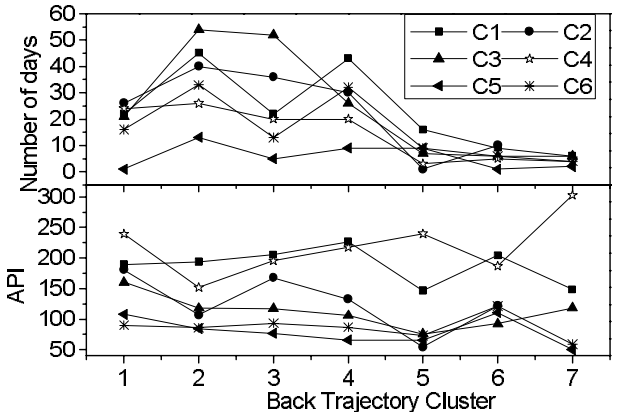

Fig. 7. Mean API values and number of days as a function of both synoptic patterns and trajectory cluster in Ürümqi.

4. Conclusions

In Ürümqi, poor meteorological conditions play a key role in heavy air pollution during the winter heating period. Synoptic classification based on wind and thermal-moisture factors and backward trajectory analyses based on the wind and pressure fields were used to assess air quality during winter heating periods in Ürümqi. PCA and a two-stage clustering (Ward's and k-means clustering) were utilized to determine six distinctive synoptic clusters that characterize the different hydrodynamic and thermodynamic conditions at the synoptic scale. The results show that synoptic classification provides a useful discriminator of air quality associated with the impact of weather situations on atmospheric tendencies for the dispersion or accumulation of air pollutants. The heaviest air-pollution episodes occurred with an extremely cold, strong anticyclone or at the front of a migrating cyclone, both with light winds, wet surface air, and relatively dry upper air. Moderate pollution was associated with the pre-cold-front and cold-front passages with lower temperatures and light winds or moderate anticyclone activity with relatively warmer, drier air. Good air quality was associated with the front of a migrating anticyclone or in a weak anticyclone with moderate winds and most warm, dry air, or the cold-front and post-cold-front passages with relatively strong northerly airflows and precipitation. As shown by backward trajectory analysis, nearly 69% of air masses influencing Ürümqi pollution levels were from the southwest; ∼22% were from the local area. There was a strong relationship between air quality and 3-day backward trajectories, which demonstrates that

longer trajectories from the southwest or short trajectories with recirculation over the study area are linked to heavy air pollution. Poor diffusion conditions, together with local circulation, enhanced air pollution, besides, long-distance air-mass transport caused serious air quality under relative good diffusion conditions.

These two approaches present an effective alternative to qualitatively forecast air quality; this comprehensive understanding of the relationships between the synoptic patterns and trajectories and the air-pollution process is important for taking measures to control and manage regional air pollution. Moreover, these results provide useful and necessary information for analyzing the impacts of weather and pollution on human health.

Acknowledgements. This work was partially supported by the National Basic Research Program (also called 973 Program) of China (Grant No. 2007CB407303), and the Knowledge Innovation Program of the Chinese Academy of Sciences (Grant No. KZCX2-YW-Q02-03).

REFERENCES

Bower, D., G. R. McGregor, D. M. Hannah, and S. C. Sheridan, 2007: Development of a spatial synoptic classification scheme for western Europe. *International Journal of Climatology,* **27**, 2017–2040.

Cape, J. N. J. Methven, and L. E. Hudson, 2000: The use of trajectory cluster analysis to interpret trace gas measurements at Mace Head, Ireland. *Atmos. Environ.*, **34**, 3651–3663

Cheng, C. S., and Coauthors, 2007: A synoptic climatological approach to assess climatic impact on air quality in South-central Canada. Part I: Historical analysis. *Water, Air, and Soil Pollution*, **182**, 131–148.

Cattell, R., 1966: The scree test for the number of factors. *Multivariate Behavioral Research,* **1**, 245–276.

Chen, Z. H., S. Y. Cheng, J. B. Li, X. R. Guo, W. H. Wang, and D. S. Chen, 2008: Relationship between atmospheric pollution processes and synoptic pressure patterns in northern China. *Atmos. Environ.,* **42**, 6078–6087.

Comrie, A., 1996: An all-season synoptic climatology of air pollution in the US-Mexico border region. *The Professional Geographer,* **48**, 237–251.

Davis, J. M., B. K. Eder, D. Nychka, and Q. Yang, 1998: Modeling the effects of meteorology on ozone in Houston using cluster analysis and generalized additive models. *Atmos. Environ.*, **32**, 2505–2520.

Davis, R. E., and L. S. Kalkstein, 1990: Development of an automated spatial synoptic climatological classification. *International Journal of Climatology*, **10**, 769–794.

Davis, R. E., and D. R. Walker, 1992: An upper-air synoptic climatology of the western United States. *Journal of Climate*, **5**, 1449–1467.

Davis, R. E., P. N. Caroline, S. Luke, M. H. David, B. K. David, P. G. Stephen, and J. S. Philip, 2010: A comparison of trajectory and air mass approaches to examine ozone variability. *Atmos. Environ.*, **44**, 64–74.

Eder, B. K., J. M. Davis, and P. Bloomfield, 1994: An automated classification scheme designed to better elucidate the dependence of ozone on meteorology. *J. Appl. Meteor.*, **33**, 1182–1199.

Eneroth, K., E. Kjellstrom, and K. Holmen, 2003: A trajectory climatology for Svalbard investigating how atmospheric flow patterns influence observed tracer concentrations. *Physics and Chemistry of the Earth*, **28**, 1191–1203.

Guo, Y. H., L. J. Gao, and A. H. Lu, 2006: Analysis of heavy air pollution episodes during typical winter ambient in Ürümqi. *Environment Chemistry*, **25**, 379–380. (in Chinese)

Huang, Z., 2005: Analysis on heavy pollution weather and meteorology factor change in Ürümqi city. *Arid Envirinmental Monitoring*, **19**, 154–157. (in Chinese)

Jolliffe, I. T., 2002: *Principal Component Analysis.* Springer-Verlag, 457pp.

Kaiser, D. P., and Y. Qian, 2002: Decreasing trends in sunshine duration over China for 1954–1998: Indication of increased haze pollution? *Geophys. Res. Lett.*, **29**(21), 2042, doi: 10.1029/2002GL016057.

Kim Oanh, N. T., P. Chutimon, W. Ekbordin, and W. Supat, 2005: Meteorological pattern classification and application for forecasting air pollution episode potential in a mountain-valley area. *Atmos. Environ.,* **39**, 1211–1225.

Lam, K. C., and S. Cheng, 1998: A synoptic climatological approach to forecast concentrations of sulfur dioxide and nitrogen oxides in Hong Kong. *Environmental Pollution*, **101**, 183–191.

Li, R., and X. Wang, 2007: Effects of precipitation on air pollution in Ürümqi City. *Desert and oasis Weather*, **1**, 13–15. (in Chinese)

Li, J., G. Z. Zhuang, K. Huang, Y. Lin, C. Xu, and S. Yu, 2008: Characteristics and sources of air-borne particulate in Ürümqi, China, the upstream area of Asia dust. *Atmos. Environ.*, **42**, 776–787.

Mamtimin, B., and F. X. Meixner, 2007: The characteristics of airpollution in the semi-arid city of Ürümqi (NW China) and its relation to climatological process. *Geophysical Research Abstracts,* **9**, 06537.

McGregor, G. R., and D. Bamzelis, 1995: Synoptic typing and its application to the investigation of weather air pollution relationships, Birmingham, United Kingdom. *Theor. Appl. Climatol.*, **51**, 223–236.

Mao, H. Y., 1997: The problems and countermeasures of sustainable development in northwest China. *Geographical Reaearch*, **16**, 12–22. (in Chinese)

State Environmental Protection Administration of China (SEPA), 1996: Ambient Air Quality Standard (GB3095-1996). Beijing, China. (in Chinese)

Sun, Y., Y. S. Wang, and C. C. Zhang, 2010: Vertical

observations and analysis of $PM_{2.5}$, O_3, and NO_x at Beijing and Tianjin from towers during summer and autumn 2006. *Adv. Atmos. Sci.*, **27**(1), 123–136, doi: 10.1007/s00376-009-8154-z.

Wang, X., Y. Ma, H. W. Wang, and Z. Y. Tao, 2002: Analysis on the Climate Characteristics of Sandstorms in North Xinjiang. *Acta Scientiarum Naturalium Universitatis Pekinens*is, **38**, 681–687. (in Chinese)

Wang, Y., and Z. Wang, 2007: The effect of air pollution in on the respiratory system diseases. *Journal of Shenyang Agricultural University* (*Social Sciences Edition*), **9**, 783–785. (in Chinese)

Wang, J., Y. Wu, and H. Liu, 2008: Primary analysis on the characteristic of the surface wind field and its influence on air pollution in Ürümqi City. *Environmental Protection of Xinjiang*, **30**, 24–28. (in Chinese)

Wu, Y., X. Wang, and C. R., Huang, 2007: Characteristic of low-level wind and its influence on air pollution in Ürümqi City. *Desert and Oasis Meteorology*, **1**, 39–41. (in Chinese)

Wu, Y., J. Wang, H. Liu, G. H. Lu, and X. H. Cui, 2008: Spatial distributions of atmospheric contaminations and effect of surface wind in Ürümqi. *Journal of Desert Research*, **28**, 986–991. (in Chinese)

Xin, J. Y., W. P. Du, Y. S. Wang, Q. X. Gao, Z. Q. Li, and M. X. Wang, 2010: Aerosol optical properties affected by a strong dust storm over central and northern China. *Adv. Atmos. Sci.,* **27**(3), 562–574, doi: 10.1007/s00376-009-9023-5.

Yang, X., Q. He, T. Liu, and L. Bai, 2010: A case analysis on the mixing layer thickness in winter over Ürümqi and its impacts to air pollution. *Desert and Oasis Meteorology*, **4**, 18–21.

Yarnal, B., 1993: *Synoptic Climatology in Environmental Analysis*. Belhaven Press, London, 195pp.

Yuan, H., G. S. Zhuang, K. A. Rahn, X. Y. Zhang, and Y. L. Li, 2006: Composition and mixing of individual particles in dust and nondust conditions of north China, spring 2002. *J. Geophys. Res.*, **111**, D20208, doi: 10.1029/2005JD006478.

Yu, T., 2000. Air pollution index for daily air quality forecasting. *Municipal Administration and Technology*, **2**, 23–26. (in Chinese)

Ziomas, I., D. Melas, C. S. Zerefos, A. F. Bais, and A. G. Paliatsos, 1995: Forecasting peak pollutant levels from meteorological variables. *Atmos. Environ.*, **29**, 3703–3711.